Structural Characterization of Layered γ-Titanium Phosphate $(C_6H_{13}NH_3)[Ti(HPO_4)(PO_4)]\cdot H_2O$

Luís Mafra, Filipe A. Almeida Paz, and João Rocha*

Department of Chemistry, CICECO, University of Aveiro, 3810-193 Aveiro, Portugal

Aránzazu Espina, Sergei A. Khainakov, and José R. García

Departamento de Química Orgánica e Inorgánica, Universidad de Oviedo, 33006 Oviedo, Spain

Christian Fernandez

Laboratoire Catalyse et Spectrochimie (CNRS UMR 6506), ENSICAEN, and Université de Caen-Basse Normandie, 14050 Caen, France

Received July 4, 2005. Revised Manuscript Received October 3, 2005

An organically templated titanium phosphate, $(C_6H_{13}NH_3)[Ti(HPO_4)(PO_4)]\cdot H_2O$, has been prepared by hydrothermal synthesis from titanium(IV) chloride, phosphoric acid, and *n*-hexylamine. The structure of this material has been characterized by powder X-ray diffraction (XRD), ^{1}H [including ^{1}H{FS−Lee−Goldburg (LG)}−^{1}H homonuclear correlation (HOMCOR), ^{1}H double quantum (DQ), and ^{1}H{FS-LG}−^{31}P cross-polarization (CP) heteronuclear correlation (HETCOR)], ^{13}C, and ^{31}P magic-angle spinning (MAS) NMR, Fourier transform infrared (FTIR) spectroscopy, and thermal analyses [thermogravimetry (TG) and differential scanning calorimetry (DSC)]. Based on the empirical evidence, particularly solid-state NMR, modeling studies, and powder XRD, a crystal structure has been proposed, having unit cell parameters $a = 5.089(2)$ Å, $b = 6.335(2)$ Å, $c = 22.792(5)$ Å, $\beta = 102.48(2)°$, space group $P2_1$, and $Z = 2$. This compound is built up of anionic titanium phosphate layers, similar to those present in the γ-type titanium phosphate, with *n*-hexylammonium cations intercalated in the interlayer space.

Introduction

Crystalline inorganic compounds were initially synthesized by traditional high-temperature methods, such as condensation,[1] chemical vapor transport,[2] vapor−liquid−solid,[3] flux,[4] and solution alloy growth.[5] However, there is an increasing interest in synthetic methods, using low or moderate temperatures (150−350 °C), that may lead to metastable compounds exhibiting unusual and useful properties. Among such methods, the hydrothermal synthetic approach is now regarded as one of the most effective.[6]

Metal salts of phosphoric acid have been known for over a century. However, research on layered metal phosphates, and their relatives, began only in the late 1950s, when some of these salts found applications as cation exchangers for the treatment of radioactive waste streams.[7] Although in an excess of phosphorus, crystalline α-zirconium phosphate may be directly obtained from zirconium(IV) and phosphoric acid solutions,[8] due to their low solubility tetravalent metal phosphates were initially prepared as amorphous gels. In 1964, Clearfield and Stynes[9] obtained the first crystalline compound, α-$Zr(HPO_4)_2\cdot H_2O$, which allowed a better understanding of their layered structure[10,11] and chemical reactivity.[12,13] Since then, these compounds have been extensively studied due to the possibility of relating their properties and crystalline structure with the many potential applications in the fields of ion exchange, intercalation, catalysis, and ion conduction.[14−18]

The preparation of layered zirconium dihydrogenophosphate-phosphate dihydrate, γ-$Zr(H_2PO_4)(PO_4)\cdot 2H_2O$, was first reported in 1968.[19] However, at that time, γ-zirconium phosphate was erroneously believed to be an isomorphous modification of the α-phase; and therefore, it was not pos-

* Address correspondence to this author. E-mail: rocha@dq.ua.pt. Telephone: +(351) 234 370 730. Fax: +(351) 234 370 084.

(1) Brenner, S. S. *The Art and Science of Growing Crystals*; Wiley: New York, 1963.
(2) Rosemberg, F. *Preparation and Characterization of Materials*; Oxford University Press: Oxford, U.K., 1987.
(3) Wagner, R. S.; Ellis, W. C.; Arnold, S. M.; Jackson, K. A. *J. Appl. Phys.* **1964**, *35*, 2993.
(4) Scheel, H. J. *Crystal Growth from High-Temperature Solutions*; Academic Press: London, 1975.
(5) Lorenz, M. R. *J. Appl. Phys.* **1962**, *33*, 3304.
(6) Rabenau, A. *Angew. Chem., Int. Ed. Engl.* **1985**, *24*, 1026.
(7) Kraus, K. A.; Phillips, H. O. *J. Am. Chem. Soc.* **1956**, *78*, 694.
(8) Trobajo, C.; Khainakov, S. A.; Espina, A.; Garcia, J. R. *Chem. Mater.* **2000**, *12*, 1787.
(9) Clearfield, A.; Stynes, J. A. *J. Inorg. Nucl. Chem.* **1964**, *26*, 117.
(10) Clearfield, A.; Smith, G. D. *Inorg. Chem.* **1969**, *8*, 431.
(11) Troup, J. M.; Clearfield, A. *Inorg. Chem.* **1977**, *16*, 3311.
(12) Kullberg, L.; Clearfield, A. *J. Phys. Chem.* **1981**, *85*, 1578.
(13) Kullberg, L.; Clearfield, A. *J. Phys. Chem.* **1981**, *85*, 1585.
(14) *Inorganic Ion Exchange Materials*; Clearfield, A., Ed.; CRC Press: Boca Raton, FL, 1982.
(15) Alberti, G.; Costantino, U. *Intercalation Chemistry*; Academic Press: New York, 1982.
(16) Alberti, G. *Recent Developments in Ion Exchange*; Elsevier Applied Science: London, 1987.
(17) Clearfield, A. *Design of New Materials*; Plenum Press: New York, 1987.
(18) Alberti, G.; Costantino, U. *Inclusion Compounds. Inorganic and Physical Aspects of Inclusion*; Oxford University Press: Oxford, U.K., 1991; Vol. 5.
(19) Clearfield, A.; Blessing, R. H.; Stynes, J. A. *J. Inorg. Nucl. Chem.* **1968**, *30*, 2249.

10.1021/cm051447f CCC: $30.25 © 2005 American Chemical Society
Published on Web 11/16/2005

sible to give a correct interpretation of the mechanism of formation and the chemical composition and structure of the isolated derivatives. Advances in the knowledge of the γ-layered structure were fundamental for the interpretation of the topotactic mechanism of formation and development of the chemistry of the γ-derivatives.[20,21]

Although only two crystalline forms of layered titanium phosphates are known, α-$Ti(HPO_4)_2 \cdot H_2O$ and γ-$Ti(H_2PO_4)(PO_4) \cdot 2H_2O$, many derivatives have been reported, including partially and completely substituted ion-exchanged forms and intercalation compounds.[22−25] Surprisingly, the γ-layered titanium phosphate is less studied than the α-phase, even though the γ-layers are more rigid, thicker, acidic, and amenable to intercalation processes. This is probably due to the fact that the structure of the γ-phase was only theoretically proposed.[26] More than a decade ago, we reported the mechanism of intercalation of *n*-alkylamines in γ-titanium phosphate, showing that 66% of the P−OH groups interact with the amine groups of the guest molecules.[23] Geometrical constraints dictate that compounds with maximum intercalation usually have the empirical formula of γ-$Ti(H_2PO_4)(PO_4) \cdot 1.3C_nH_{2n+1}NH_2 \cdot H_2O$ (with $n = 1-6$), and crystalline phases with lower amine content can also be isolated.

The hydrothermal synthesis of a γ-titanium phosphate intercalation compound, $Ti_2(HPO_4)_2(PO_4)_2 \cdot C_2N_2H_{10}$, has been recently reported,[27] and only one other member of this family is known, $Ti_2(H_2PO_4)(HPO_4)(PO_4)_2 \cdot 0.5C_6N_2H_{16}$.[28] Although monoalkylamines are usually employed as templates for the synthesis of titanium phosphate metastable phases, the preparation of a γ-titanium phosphate alkylamine-intercalated compound has never been reported to date. Here, we describe the hydrothermal synthesis and structural characterization of the first member in this family, $(C_6H_{13}NH_3)[Ti(HPO_4)(PO_4)] \cdot H_2O$. Because of strong preferential orientation effects and thermal disorder of the alkyl chains of the *n*-hexylammonium cations in the interlayer space, solving the structure of this material from only powder X-ray diffraction (XRD) evidence proved to be a very difficult task, and thus, a comprehensive solid-state NMR study has been performed. NMR has been used ab initio to inform the XRD and modeling work and, at the final stage, to confirm the obtained crystal structure.

Experimental Section

Synthesis. Hydrothermal synthesis of $(C_6H_{13}NH_3)[Ti(HPO_4)(PO_4)] \cdot H_2O$ (yield >90%) was carried out in a stainless steel Teflon-lined vessel (designed and manufactured at Oviedo University) under autogenous pressure. *n*-Hexylamine (Merck, purity >98%), 85% H_3PO_4 (Merck), and $TiCl_4$ (Merck, purity >99%) were mixed in the molar ratio 1:10:10 ($TiCl_4$:H_3PO_4:$C_6H_{13}NH_2$) in a total volume of ca. 40 cm^3. The reaction vessel was sealed and heated to 185 °C for 10 days. The obtained solid was filtered off, washed with an excess of distilled water, and dried in air at ambient temperature.

Table 1. Crystal Data of $(C_6H_{13}NH_3)[Ti(HPO_4)(PO_4)] \cdot H_2O$

formula	$C_6NH_{19}TiP_2O_9$
formula weight	359.11
crystal system	monoclinic
space group	$P2_1$ (no. 4)
a/Å	5.089(2)
b/Å	6.335(2)
c/Å	22.792(5)
β/deg	102.48(2)
Z	2
R_p	0.200
R_{wp}	0.227
R_F	0.210
χ^2	5.8

Intercalation was tested by placing the isolated material in an atmosphere with *n*-hexylamine vapor at ambient temperature for 60 days. The solid obtained was air-dried at 50 °C and stored in a desiccator on top of an aqueous solution of 50% H_2SO_4.

Instrumentation. The phosphorus and titanium contents were determined with a SpectraSpectrometer inductively coupled plasma mass spectrometer (ICP-MS) after a weighed amount of the sample was dissolved in aqueous HF. Microanalytical data (C and N) were obtained with a Perkin-Elmer 2400B elemental analyzer. Thermal analyses were performed under nitrogen atmosphere (heating rate ca. 10 °C min^{-1}) in a Mettler TA4000 (TG 50 and DSC 30) model. Infrared spectra were recorded with a Perkin-Elmer 1000 FT-IR spectrophotometer from KBr pellets. Micrographs were recorded with a JEOL JSM-6100 electron microscope operating at 20 kV.

Powder X-ray diffraction (XRD) patterns were collected on a conventional powder diffractometer Philips 3040 with graphite-monochromatized Cu Kα radiation ($\lambda = 1.5418$ Å), operating in the Bragg−Brentano ($\theta/2\theta$) geometry. The sample was gently ground in an agate mortar and side-loaded into a holder to minimize the orientation effects, and data were collected at ambient temperature over the angular range 3−110° 2θ, with a step of 0.02° and a counting time of 10 s/step.

Chemical composition suggested a structure with an inorganic component related to that of the γ-titanium phosphate. As a starting set for the structural model, the coordinates reported for γ-$Ti(H_2PO_4)(PO_4) \cdot 2H_2O$,[26,29] were used and the refinement was carried out in space group $P2_1$ (no. 4) by use of GSAS.[30] Crystallographic parameters are summarized in Table 1, fractional atomic coordinates in Table 2, selected bond lengths and angles in Table 3, and short (N,O)···O contacts related to hydrogen bonds in Table 4.

^1H, ^{13}C, and ^{31}P NMR spectra have been recorded at 9.4 T on a Bruker Avance 400 spectrometer (DSX model) on 4 and 2.5 mm (up to 30 kHz spinning rate) double-bearing probes at, respectively, 400.11, 100.62, and 161.97 MHz. In 2D ^1H\{FS−Lee−Goldburg (LG)\}−^1H homonuclear correlation (HOMCOR) experiments, the sample was restricted to the center of a 4-mm ZrO_2 rotor. Chemical shifts are quoted in parts per million (ppm) from tetramethylsilane (TMS) (^1H and ^{13}C) and 85% H_3PO_4 (^{31}P). ^1H and ^{31}P single-pulse NMR spectra have been recorded with, respectively, spinning rates of 30 and 10 kHz, 60 and 4 s recycle delays, and 45° pulses.

(20) Poojary, D. M.; Shpeizer, B.; Clearfield, A. *J. Chem. Soc., Dalton Trans.* **1995**, 111.
(21) Alberti, G. *Comprehensive Supramolecular Chemistry*; Pergamon Press: Oxford, U.K., 1996.
(22) Llavona, R.; Suarez, M.; Garcia, J. R.; Rodriguez, J. *Inorg. Chem.* **1989**, *28*, 2863.
(23) Menendez, A.; Barcena, M.; Jaimez, E.; Garcia, J. R.; Rodriguez, J. *Chem. Mater.* **1993**, *5*, 1078.
(24) Espina, A.; Garcia, J. R.; Guil, J. M.; Jaimez, E.; Parra, J. B.; Rodriguez, J. *J. Phys. Chem. B* **1998**, *102*, 1713.
(25) Espina, A.; Jaimez, E.; Khainakov, S. A.; Trobajo, C.; Garcia, J. R.; Rodriguez, J. *Chem. Mater.* **1998**, *10*, 2490.
(26) Christensen, A. N.; Andersen, E. K.; Andersen, I. G. K.; Alberti, G.; Nielsen, M.; Lehmann, M. S. *Acta Chem. Scand.* **1990**, *44*, 865.
(27) Serre, C.; Taulelle, F.; Ferey, G. *Solid State Sci.* **2001**, *3*, 623.
(28) Chen, C.; Yang, Y. L.; Huang, K. L.; Sun, Z. H.; Wang, W.; Yi, Z.; Liu, Y. L.; Pang, W. Q. *Polyhedron* **2004**, *23*, 3033.
(29) Salvado, M. A. Ph.D. Thesis. University of Oviedo, Oviedo, Spain, 1999.
(30) Larson, A. C.; Von Dreele, R. B. *General Structure Analysis System* (*GSAS*); Los Alamos National Laboratory Report LAUR 86-748; 2000.

Table 2. Fractional Atomic Coordinates of $(C_6H_{13}NH_3)[Ti(HPO_4)(PO_4)]\cdot H_2O$

	x	*y*	*z*
Ti(1)	0.802(1)	0.250(1)	0.068(1)
P(1)	0.221(1)	0.238(1)	−0.033(1)
P(2)	0.378(1)	0.140(1)	0.163(1)
O(1)	0.989(1)	0.238(1)	0.000(1)
O(2)	0.791(1)	0.552(1)	0.073(1)
O(3)	0.791(1)	−0.064(1)	0.071(1)
O(4)	0.498(1)	0.239(1)	0.007(1)
O(5)	0.126(1)	0.248(1)	0.130(1)
O(6)	0.626(1)	0.206(1)	0.140(1)
O(7)	0.325(1)	0.897(1)	0.151(1)
O(8)	0.451(1)	0.162(1)	0.235(1)
O(W)	0.421(1)	0.347(1)	0.341(1)
N(1)	0.749(1)	0.581(1)	0.193(1)
C(1)	0.749(1)	0.581(1)	0.258(1)
C(2)	0.749(1)	0.786(1)	0.291(1)
C(3)	0.749(1)	0.786(1)	0.358(1)
C(4)	0.749(1)	0.991(1)	0.392(1)
C(5)	0.749(1)	0.991(1)	0.459(1)
C(6)	0.749(1)	0.195(1)	0.492(1)

Table 3. Selected Bond Lengths and Angles of $(C_6H_{13}NH_3)[Ti(HPO_4)(PO_4)]\cdot H_2O$[a]

Ti(1)−O(1)	1.99(2)	O(1)−Ti(1)−O(2)	96.3(2)
Ti(1)−O(2)	1.92(1)	O(1)−Ti(1)−O(3)	90.6(2)
Ti(1)−O(3)	1.99(2)	O(1)−Ti(1)−O(4)	82.9(1)
Ti(1)−O(4)	1.84(1)	O(1)−Ti(1)−O(5)[b]	95.4(2)
Ti(1)−O(5)[b]	1.93(1)	O(1)−Ti(1)−O(6)	169.7(3)
Ti(1)−O(6)	2.06(3)	O(2)−Ti(1)−O(3)	173.1(2)
P(1)−O(1)[c]	1.53(1)	O(2)−Ti(1)−O(4)	93.0(1)
P(1)−O(2)[d]	1.48(2)	O(2)−Ti(1)−O(5)[b]	89.7(1)
P(1)−O(3)[e]	1.52(1)	O(2)−Ti(1)−O(6)	93.7(1)
P(1)−O(4)	1.50(1)	O(3)−Ti(1)−O(4)	87.9(1)
P(2)−O(5)	1.50(1)	O(3)−Ti(1)−O(5)[b]	89.7(1)
P(2)−O(6)	1.53(1)	O(3)−Ti(1)−O(6)	79.4(2)
P(2)−O(7)	1.58(3)	O(4)−Ti(1)−O(5)[b]	177.0(1)
P(2)−O(8)	1.61(4)	O(4)−Ti(1)−O(6)	99.1(2)
N(1)−C(1)	1.50(1)	O(6)−Ti(1)−O(5)[b]	82.2(2)
C(1)−C(2)	1.50(1)	P(1)−O(4)−Ti(1)	168.7(1)
C(2)−C(3)	1.53(1)	P(2)−O(6)−Ti(1)	148.1(1)
C(3)−C(4)	1.51(1)	O(1)[c]−P(1)−O(2)[d]	111.6(1)
C(4)−C(5)	1.53(1)	O(1)[c]−P(1)−O(3)[e]	109.9(1)
C(5)−C(6)	1.50(1)	O(1)[c]−P(1)−O(4)	115.1(1)
		O(2)[d]−P(1)−O(3)[e]	108.3(2)
N(1)−C(1)−C(2)	119.3(2)	O(2)[d]−P(1)−O(4)	106.5(1)
C(1)−C(2)−C(3)	119.3(2)	O(3)[e]−P(1)−O(4)	105.0(1)
C(2)−C(3)−C(4)	120.8(1)	O(5)−P(2)−O(6)	112.5(1)
C(3)−C(4)−C(5)	120.8(1)	O(5)−P(2)−O(7)	105.2(2)
C(4)−C(5)−C(6)	120.2(1)	O(5)−P(2)−O(8)	117.1(3)
		O(6)−P(2)−O(7)	109.3(2)
		O(6)−P(2)−O(8)	107.5(2)
		O(7)−P(2)−O(8)	104.8(4)

[a] Bond lengths are given in angstroms; bond angles are given in degrees. [b] Symmetry code used to generate equivalent atoms: $(1 + x, y, z)$. [c] $(-1 + x, y, z)$. [d] $(1 - x, -^1/_2 + y, -z)$. [e] $(1 - x, ^1/_2 + y, -z)$.

Table 4. Short (N,O)···O Contacts in $(C_6H_{13}NH_3)[Ti(HPO_4)(PO_4)]\cdot H_2O$[a]

N(1)···O(2)	2.80(1)	O(7)···O(3)[b]	2.94(2)
N(1)···O(6)	2.68(3)	O(1W)···O(8)	2.72(3)
N(1)···O(7)[c]	2.95(2)		

[a] Contacts are given in angstroms. [b] Symmetry code used to generate equivalent atoms: $(-1 + x, 1 + y, z)$. [c] $(x, 1 + y, z)$.

$^1H-^{13}C$ and $^1H-^{31}P$ cross-polarization (CP)/magic-angle spinning (MAS) NMR spectra were recorded with, respectively, spinning rates of 4.5 and 10 kHz, a recycle delay of 4 s, a ^1H 90° pulse of 3.5 μs, and contact times in the range 100 μs−2 ms. The ^1H double-quantum (DQ) MAS NMR experiment was performed with the improved version of the back-to-back (BABA) sequence proposed by Feike et al.[31] The excitation/reconversion block has a duration of an integral number of two rotor periods where resonance offsets and CSA are averaged out in the zero-order average Hamiltonian. The excitation/ reconversion block has the following form:

$$\frac{\Delta}{2}-\left(\frac{\pi}{2}\right)_x-\tau-\left(\frac{\pi}{2}\right)_x-\Delta-\left(\frac{\pi}{2}\right)_y-\tau-\left(\frac{\pi}{2}\right)_{-y}-\Delta-\left(\frac{\pi}{2}\right)_x-\tau-\left(\frac{\pi}{2}\right)_x-\Delta-\left(\frac{\pi}{2}\right)_{-y}-\tau-\left(\frac{\pi}{2}\right)_y-\frac{\Delta}{2}$$

where $\tau = \tau_R/2$ minus half the pulse lengths, with τ_R denoting a rotor period. Here, the duration of the excitation and reconversion block was set to two rotor periods, 66 μs. After the reconversion, a *z*-filter time of nine rotor periods (9 × 33 μs) was employed to dephase any transversal magnetization. A final 90° pulse was used to create transverse magnetization and for signal detection. The total phase cycle consisted of 16 steps (four steps to select $p = \pm 2$ after the excitation sequence and four steps to select $p = 0 \rightarrow p = -1$). A total of 192 t_1 points with 16 transients each were acquired by use of t_1 increments synchronized with the rotor period. Sign discrimination was achieved in the F1 dimension by the time-proportional phase incrementation (TPPI) method by incrementing the phase of the excitation pulses by 45°. The train of 90° pulses in the BABA sequence was set to 2.5 μs.

In all experiments with FS-LG homonuclear decoupling, the proton radio frequency (rf) field amplitude was set to ca. 83 kHz. The phase switching between each Lee−Goldburg (LG) pulse was optimized on the multiplet structure of adamantane. In the optimization of the FS-LG decoupling power, multiple 2D experiments were recorded by use of natural abundance alanine and monitoring the spectral resolution in the F1 dimension. Before each LG pulse, the frequency offset was alternated between +ΔLG and −ΔLG (or $\pm\nu_1/\sqrt{2}$) corresponding to $+58\,925 + \nu_{lg}$ Hz and $-58\,925 + \nu_{lg}$ Hz. Best results are obtained by use of asymmetric offsets during FS-LG decoupling of about $\nu_{lg} = \pm 1-5$ kHz.[32] This value is added to the frequency jumps described above and is optimized to shift the spectrum out of the axial artifact centered at the middle of the F1 dimension, thus avoiding inconvenient spectral interference. The LG pulse length (τ_{LG}) was set to 9.8 μs and, as a consequence, one FS-LG unit equals two successive τ_{LG} units. Quadrature detection in t_1 was achieved by the States-TPPI method.[33] In theory, under FS-LG decoupling the ^1H chemical shift is scaled by $1/\sqrt{3}$ (ca. 0.57). The correct ^1H chemical shifts and the scaling factor λ of the FS-LG dimension (F1) of HOMCOR/heteronuclear correlation (HETCOR) spectra were determined by comparison with the 1D ^1H spectra recorded under fast MAS (30 kHz). Scaling factors of 0.56−0.58 were obtained for all spectra. The FS-LG decoupling blocks employed during the homonuclear decoupling were based on ref 34. Specific experimental conditions for each spectrum are given in the figure captions.

Results and Discussion

The first (and dominant) reflection of the powder XRD pattern of the title compound corresponds to a *d*-spacing of ca. 22.2 Å (Figure 1a). The treatment of this compound with mineral acids (e.g., 0.1 M HNO_3) yields γ-titanium phosphate, $Ti(H_2PO_4)(PO_4)\cdot 2H_2O$ (Figure 2a),[26,35] strongly suggesting that the material possesses an inorganic lattice related to that of the γ-layered structure. According to elemental composition studies and thermal analyses (Table 5), the

(31) Feike, M.; Demco, D. E.; Graf, R.; Gottwald, J.; Hafner, S.; Spiess, H. W. *J. Magn. Reson., Ser. A* **1996**, *122*, 214.
(32) Lesage, A.; Sakellariou, D.; Steuernagel, S.; Emsley, L. *J. Am. Chem. Soc.* **1998**, *120*, 13194.
(33) States, D. J.; Haberkorn, R. A.; Ruben, D. J. *J. Magn. Reson.* **1982**, *48*, 286.
(34) van Rossum, B. J.; Forster, H.; deGroot, H. J. M. *J. Magn. Reson.* **1997**, *124*, 516.

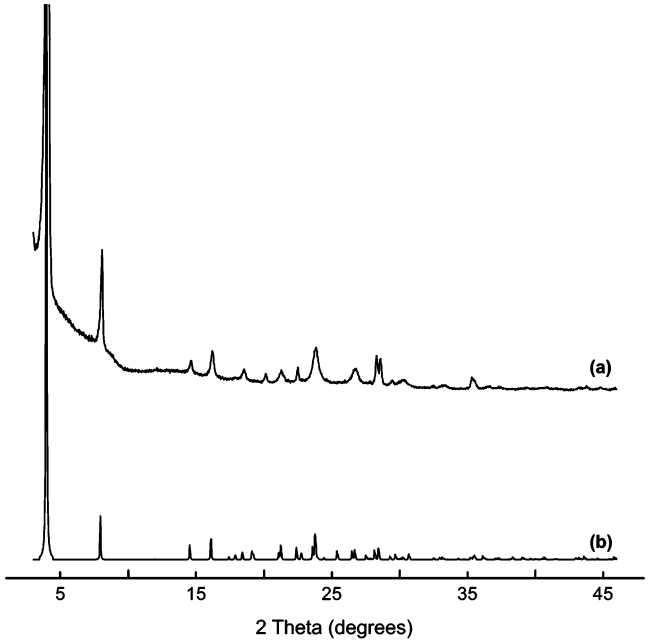

Figure 1. (a) Experimental and (b) simulated powder XRD patterns of $(C_6H_{13}NH_3)[Ti(HPO_4)(PO_4)]\cdot H_2O$.

chemical composition of the new titanium phosphate is consistent with the $(C_6H_{13}NH_3)[Ti(HPO_4)(PO_4)]\cdot H_2O$ empirical formula. We note that when *n*-hexylamine ($C_6H_{13}NH_2$) inclusion occurs, there is proton transfer from the acidic hydrogenophosphate moieties in the γ-titanium phosphate layers to the amine group, thus leading to the presence of *n*-hexylammonium cations ($C_6H_{13}NH_3^+$) in the interlayer spaces (shown by solid-state NMR studies, see below).

Thermogravimetry gives a total weight loss from ambient temperature to 800 °C of ca. 36.0% (see Supporting Information), consistent with a stoichiometric residue of TiP_2O_7 (calculated 38.2%). Differential thermogravimetry (DTG) and differential scanning calorimetry (DSC) curves show a complex thermal decomposition process, with three partially overlapping steps. The first weight loss, at 50−200 °C, corresponds to the release of a water molecule per formula unit (observed ca. 5.9%, calculated 5.0%). The following two weight losses (at 200−490 and 490−700 °C) correspond to the removal of the *n*-hexylamine (observed ca. 25.2%, calculated 28.1%) and to the release of structural water from the condensation of hydrogenophosphate groups (observed ca. 4.9%, calculated 5.0%). Heating the sample at ca. 150 °C, followed by stabilization in air, did not change the powder XRD pattern or the elemental analysis (Figures 1a and 2b and Table 5). The corresponding decomposition route is as follows:

$$(C_6H_{13}NH_3)[Ti(HPO_4)(PO_4)]\cdot H_2O(s) \rightarrow (C_6H_{13}NH_3)[Ti(HPO_4)(PO_4)](s) + H_2O(g)$$

$$(C_6H_{13}NH_3)[Ti(HPO_4)(PO_4)](s) \rightarrow Ti(H_2PO_4)(PO_4)(s) + C_6H_{13}NH_2(g)$$

$$Ti(H_2PO_4)(PO_4)(s) \rightarrow TiP_2O_7(s) + H_2O(g)$$

(35) Gonzalez, E.; Llavona, R.; Garcia, J. R.; Rodriguez, J. *J. Chem. Soc., Dalton Trans.* **1989**, 1825.

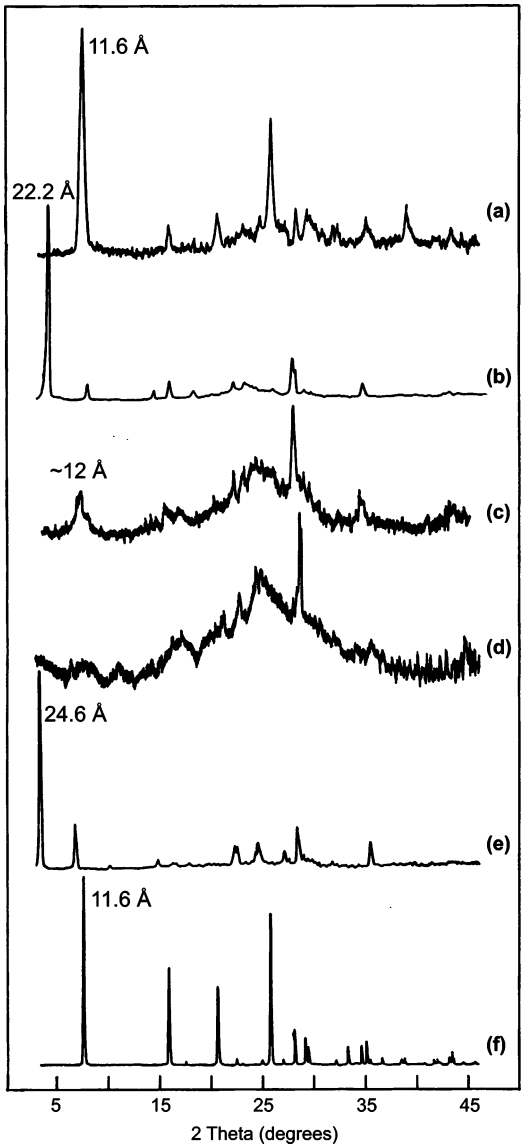

Figure 2. Powder XRD patterns of $(C_6H_{13}NH_3)[Ti(HPO_4)(PO_4)]\cdot H_2O$: (a) treated with 0.1 M HNO_3, then calcined at (b) 150, (c) 350, and (d) 400 °C (and subsequently stabilized in air at room temperature), or (e) stabilized at room temperature in a saturated atmosphere of *n*-hexylamine for 60 days. For comparison, the simulated powder XRD pattern of γ-titanium phosphate, $Ti(H_2PO_4)(PO_4)\cdot 2H_2O$, is also shown (f).[26]

Intercalates with lower amine content have been isolated by thermal treatment. Heating up the title compound to ca. 350 °C leads to the formation of the $(C_6H_{13}NH_3)_{0.3}[Ti(H_{1.7}PO_4)(PO_4)]$ phase (Figure 2c; Table 5), characterized by an interlayer spacing of ca. 12 Å, suggesting an arrangement of the ammonium residues nearly parallel to the phosphate layer. When the material is calcined at ca. 400 °C, an amorphous solid is obtained (Figure 2d). The carbon content of this phase indicates that the release of the organic residues is not complete (Table 5), with the residue having an empirical formula of $(C_6H_{13}NH_3)_{0.2}[Ti(H_{1.8}PO_4)(PO_4)]$.

Scanning electron microscopic (SEM) images of $(C_6H_{13}NH_3)[Ti(HPO_4)(PO_4)]\cdot H_2O$ (see Supporting Information) show that the particles are circular plate aggregates with a diameter of ca. 2−8 μm, and the combination with powder XRD further indicates that these plates have an average dimension, perpendicular to the basal plane, of ca. 0.3 μm.

Table 5. Analytical Data and Weight Loss at 800 °C for Intercalation Compounds

formula	exptl (%)					calcd (%)				
	Ti	P	C	N	weight loss	Ti	P	C	N	weight loss
$(C_6H_{13}NH_3)[Ti(HPO_4)(PO_4)]\cdot H_2O$[a]	12.7	16.9	19.7	3.8	36.0	13.3	17.3	20.1	3.9	38.2
$(C_6H_{13}NH_3)[Ti(HPO_4)(PO_4)]\cdot H_2O$[b]	12.8	17.0	19.6	3.7	36.8	13.3	17.3	20.1	3.9	38.2
$(C_6H_{13}NH_3)_{0.3}[Ti(H_{1.7}PO_4)(PO_4)]$[c]	17.5	22.3	7.3	1.4	18.1	17.7	23.0	8.0	1.6	17.9
$(C_6H_{13}NH_3)_{0.2}[Ti(H_{1.8}PO_4)(PO_4)]$[d]	18.0	23.1	5.2	1.0	14.1	18.7	23.8	5.5	1.1	14.7
$(C_6H_{13}NH_3)[Ti(HPO_4)(PO_4)]\cdot 0.3C_6H_{13}NH_2\cdot H_2O$[e]	11.9	15.5	24.6	4.6	43.7	12.2	15.8	24.4	4.7	43.4

[a] Sample obtained by hydrothermal synthesis and stabilization at room temperature. [b] Sample thermally treated (1 day) at 150 °C. [c] Sample thermally treated (1 day) at 350 °C. [d] Sample thermally treated (1 day) at 400 °C. [e] Sample obtained by solid−vapor contact of starting sample with *n*-hexylamine (60 days).

SEM inspection of samples treated at high temperature reveals that the particle morphology does not change.

The Fourier transform infrared (FTIR) spectrum of the title material (see Supporting Information) shows a strong band centered at 982 cm^{-1} with the shoulders at 1236 and 1155 cm^{-1}, attributed to the various (symmetric and antisymmetric) stretching (υ) P−O vibrational modes of the phosphate groups together with the presence of C−N stretching vibrations. The presence of the water molecule of crystallization involved in hydrogen bonding with the neighboring moieties is confirmed by the stretching (υ) O−H (ca. 3414 cm^{-1}) and the in-plane (δ_s) H−O−H deformation (ca. 1622 cm^{-1}) vibrational modes. The *n*-hexylammonium cations give the symmetric (ca. 2859 cm^{-1}) and antisymmetric (ca. 2957, 2930 cm^{-1}) stretching (υ) modes from the -CH_2- alkyl chains, and also the bands at ca.1520 and 2450 cm^{-1} attributed to the N−H in-plane deformation (δ_s) and stretching (υ), respectively, of the protonated amine group. A typical methylene rocking (ρ) vibration, in which all of the methylene groups rock in phase, appears as a medium-intensity band at ca. 700 cm^{-1}. The -CH_2- groups further display a sharp scissoring (δ_s) band near ca. 1400 cm^{-1}.

When $(C_6H_{13}NH_3)[Ti(HPO_4)(PO_4)]\cdot H_2O$ is stored in an atmosphere saturated with *n*-hexylamine, a new crystalline phase with an interlayer distance of ca. 24.6 Å is isolated (Figure 2e). Morphological studies indicate that the intercalation process occurs smoothly without change of the particle morphology (see Supporting Information). This *d*-spacing was previously observed in a material obtained by solid−vapor contact of γ-titanium phosphate with *n*-hexylamine, $(C_6H_{13}NH_3)[Ti(HPO_4)(PO_4)]\cdot 0.3(C_6H_{13}NH_2)\cdot H_2O$,[23] and elemental composition studies (Table 5) confirm the presence of the same phase.

To propose a possible structural model for $(C_6H_{13}NH_3)[Ti(HPO_4)(PO_4)]\cdot H_2O$, compatible with the experimental data, modeling studies based on powder XRD data were carried out. From the very beginning, the solid-state NMR evidence described (for convenience) below was available and was taken into consideration when the model was built up.

(1) A list of peak positions was obtained from the powder X-ray raw data by use of XFIT.[36] Indexing was performed with TREOR and KOHL, which are included in the CRYSFIRE suite.[37] A monoclinic cell with $a = 5.18$ Å, $b = 6.31$ Å, $c = 22.84$ Å, and $\beta = 104.7°$ ($M_{19} = 20$) was found. The indexed reflections showed systematic absences of the type $0k0$, $k = 2n + 1$, indicating that the space group is either $P2_1$ or $P2_1/m$.

(2) Since the *a* and *b* parameters were very similar to those of γ-titanium phosphate ($a = 5.181$ Å and $b = 6.347$ Å),[26]

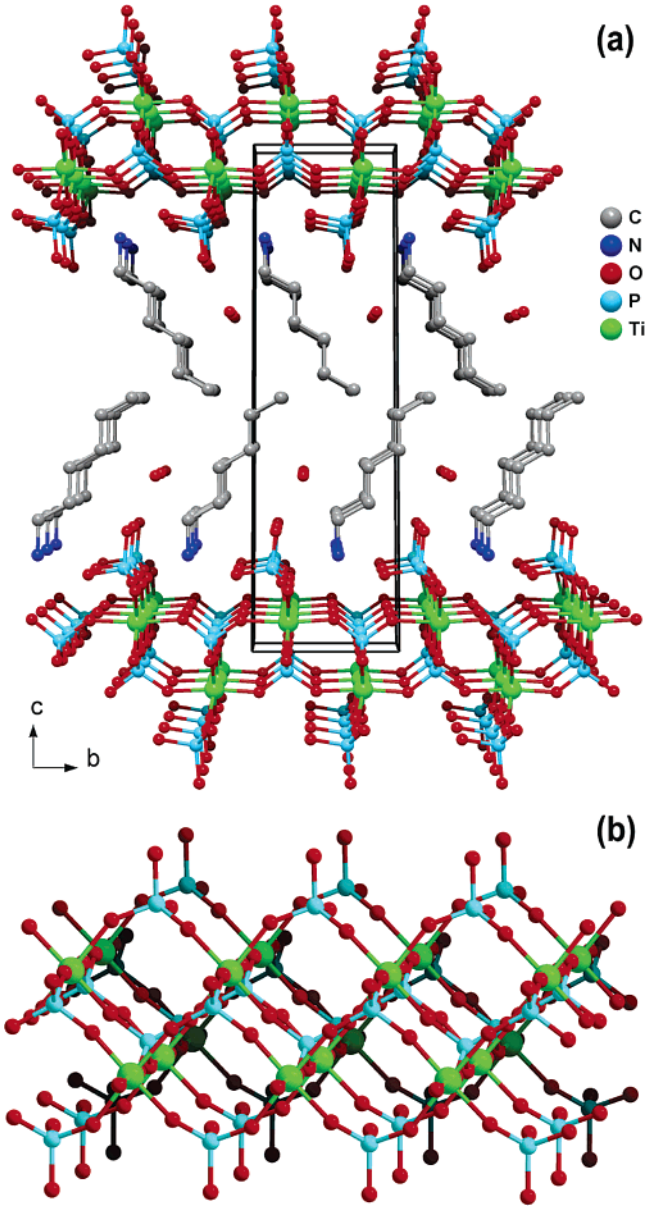

Figure 3. (a) Proposed crystal structure of $(C_6H_{13}NH_3)[Ti(HPO_4)(PO_4)]\cdot H_2O$ viewed along the [1 0 0] direction. (b) Perspective view of the two-dimensional $[Ti(HPO_4)(PO_4)]^-$ anionic sheet.

(36) Cheary, R. W.; Coelho, A. A. *XFIT*; Deposited in CCP14 Powder Diffraction Library, Engineering and Physical Sciences Research Council; Daresbury Laboratory: Warrington, England, 1997.

(37) Shirley, R. *The CRYSFIRE System for Automatic Powder Indexing: User's Manual*; Lattice Press: Guildford, Surrey, England, 2000.

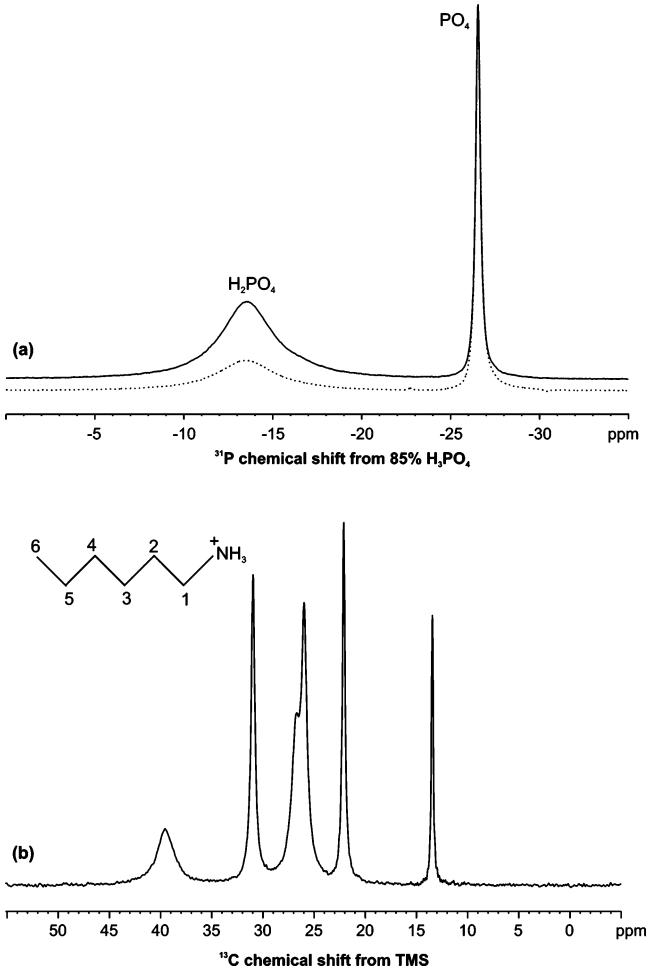

Figure 4. (a) ^{31}P MAS (dotted line), ^{1}H−^{13}P CP/MAS (continuous line, CT = 500 μs) and (b) ^{1}H−^{13}C CP/MAS NMR spectra (CT = 1500 μs) of $(C_6H_{13}NH_3)[Ti(HPO_4)(PO_4)]\cdot H_2O$.

it was assumed that the inorganic backbone of the layer is of γ type. When the γ-titanium phosphate *a*, *b*, and β are kept constant (refined in the $P2_1$ space group because the refinement in the $P2_1/m$ group did not progress appropriately, $R_{wp} = 0.340$), and with the known experimental interlayer distance of the intercalation compound, a monoclinic cell ($a = 5.181$ Å, $b = 6.347$ Å, $c = 22.75$ Å, $\beta = 102.59°$) was obtained.

(3) After the γ-titanium phosphate inorganic layers were displaced by the interlayer spacing of the intercalation compound, the initial atomic coordinates for the P, Ti, and O atoms were estimated by use of ATOMS.[38]

(4) GSAS[30] was used to refine the unit cell parameters (Table 1) and the starting structure model by assuming that the C−N bond is perpendicular to the *ab* plane and that the alkyl chains have a trans−trans conformation with bond lengths and angles identical to those of a crystalline *n*-paraffin.[39] Thermal parameters were refined isotropically ($U_{iso} = 0.025$), and a March−Dollase[40,41] correction along the 00*l* direction was applied for preferred orientations.

Final atomic coordinates and selected bond lengths and angles for the refined model are collected in Tables 2 and 3,

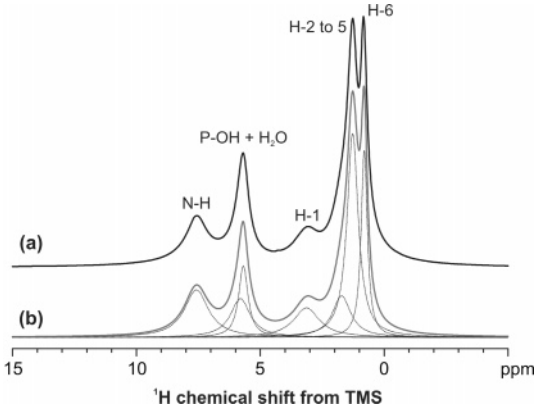

Figure 5. ^{1}H MAS NMR spectrum of $(C_6H_{13}NH_3)[Ti(HPO_4)(PO_4)]\cdot H_2O$ recorded with a 30 kHz spinning rate. The (a) experimental and (b) simulated and individual simulation peaks are also depicted.

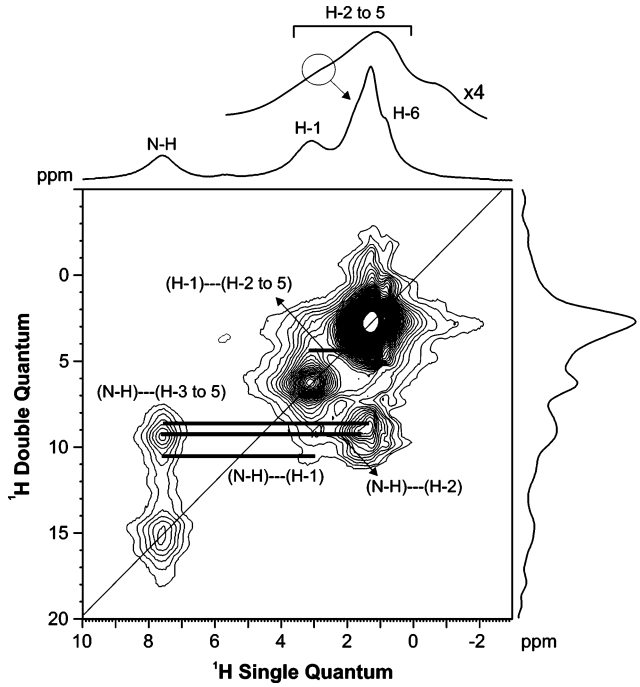

Figure 6. ^{1}H DQ MAS spectrum of $(C_6H_{13}NH_3)[Ti(HPO_4)(PO_4)]\cdot H_2O$ acquired with a spinning rate of 30 kHz. The DQ excitation time (τ_{exc}) and reconversion time (τ_{rec}) was set to 66 μs.

respectively. This model produces a simulated powder XRD pattern that is in good agreement with the experimental pattern (Figure 1). Differences in intensity are most probably due to the preferential orientation of the crystallites and thermal disorder of the alkyl chains of the interlayer *n*-hexylammonium cations. At this point, it is important to stress that, despite the modest figures of merit (Table 1), the crystal model is fully supported by all empirical evidence available, particularly the NMR data discussed below.

The structures of $(C_6H_{13}NH_3)[Ti(HPO_4)(PO_4)]\cdot H_2O$ (Figure 3a) and γ-titanium phosphate[26] are similar. Individual two-dimensional anionic $[Ti(HPO_4)(PO_4)]^-$ sheets are constructed by corner-sharing four-ring chains formed by $\{PO_4\}$ tetrahedra and $\{TiO_6\}$ octahedra (Figure 3b). The Ti−O, P−O, O−Ti−O, and O−P−O bond lengths and angles (Table 3) are typical and in good agreement with the values

(38) www.shapesoftware.com.
(39) Fabry, J.; Petricek, V.; Kroupa, J.; Cisarova, I. *Acta Crystallogr. B* **2000**, *56*, 906.
(40) March, A. *Z Kristallogr.* **1932**, *81*, 285.
(41) Dollase, W. A. *J. Appl. Crystallogr.* **1986**, *19*, 267.

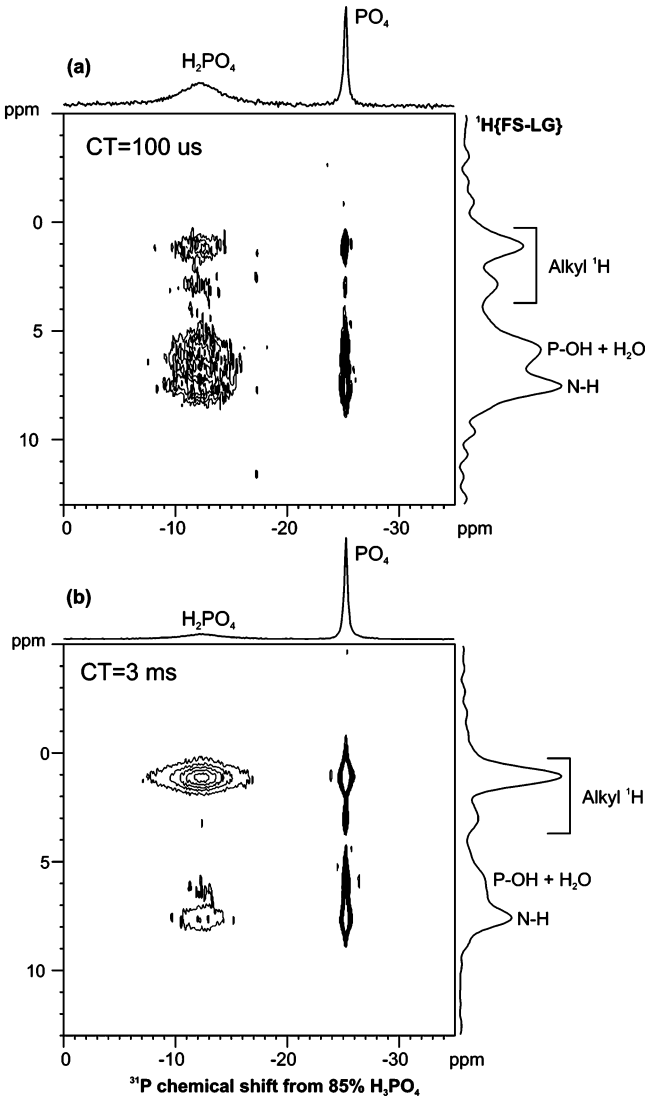

Figure 7. $^{1}H\{FS\text{-}LG\}-^{31}P$ CP HETCOR NMR spectra of $(C_6H_{13}NH_3)[Ti(HPO_4)(PO_4)]\cdot H_2O$ recorded with contact times of (a) 100 μs and (b) 3000 μs. A total of 128 t_1 increments with 16 transients each were collected. In all experiments the F1 increments were synchronized with an integral number of FS-LG units, $n(2t_{LG})$, with $n = 3$. The recycle delay was set to 3 s. The value of ν_{lg} employed was −5000 Hz.

reported for other titanium phosphates.[27,28] The structure contains two kinds of phosphate groups: PO_4^{3-} sharing their oxygen atoms with titanium centers, and HPO_4^{2-} having two bridging and two terminal oxygen atoms. These terminal HPO_4^{2-} groups are connected to the chains and point toward the interlayer region, directly interacting with the protonated amine groups from neighboring *n*-hexylammonium cations through hydrogen bonds (Table 4).

Solid-state NMR confirms and further elucidates the details of the proposed crystal structure. The ^{31}P MAS NMR spectrum of $(C_6H_{13}NH_3)[Ti(HPO_4)(PO_4)]\cdot H_2O$ exhibits two resonances at ca. −13.5 and −26.5 ppm in a 1:1 intensity (area) ratio (Figure 4a), in accord with the proposed crystal structure, which calls for the presence of two types of ^{31}P local environments. The peak at −13.5 ppm is much enhanced upon $^{1}H-^{31}P$ cross-polarization and is, thus, assigned to the HPO_4^{2-} site (Figure 4a). The $^{1}H-^{13}C$ CP/MAS spectrum (Figure 4b) displays six resonances at ca. 13.4, 22.1, 26.0, 26.7, 31.0, and 39.6 ppm attributed to C-6, C-5, C-3, C-4, C-2, and C-1, respectively, thus fully supporting the proposed crystal structure. In particular, NMR indicates that intercalated *n*-hexylamine is protonated and that there is a single type of *n*-hexylammonium cation in the unit cell. The ^{1}H MAS (30 kHz spinning rate, Figure 5) and $^{1}H\{FS\text{-}LG\}-^{1}H$ HOMCOR (see Supporting Information) NMR spectra of the title material exhibit five resonances. Deconvolution of the former spectrum requires a total of seven peaks, five of which are attributed to the *n*-hexylammonium ion: 0.8 ppm (relative area 1.5), H-6; 1.3 ppm (3), H-3−5; 1.7 ppm (1), H-2; 3.1 ppm (1), H-1; and 7.6 ppm (1.5), N−H. The remaining resonance has been deconvoluted with two peaks, at 5.7 ppm (0.9), attributed to water molecules, and 5.8 ppm (1), P−OH groups. Indeed, upon sample dehydration (ca. 150 °C, 24 h), the intensity of the former decreases considerably (not shown). The ^{1}H double-quantum BABA spectrum (Figure 6) further confirms the integrity of the *n*-hexylammonium cation in the interlayer space. Importantly, the H_2O and P−OH resonances at ca. 5.7 ppm virtually disappear from the diagonal of the spectrum, which can probably be attributed to fast ^{1}H exchange involving water molecules or the N−H groups from the *n*-hexylammonium cations and neighboring P−OH groups, and also to some mobile lattice water.

Consider now the $^{1}H-^{31}P$ HETCOR NMR spectrum of the as-prepared sample (Figure 7) and its F1 cross-sections (Figure 8). At relatively short contact times (100 μs) the H_2O, P−OH, and N−H proton resonances dominate the spectrum, while at long contact times (3 ms) the H-1−6 ^{1}H peaks are considerably enhanced. Again, these observations support the proposed crystal structure because they indicate that H_2O,

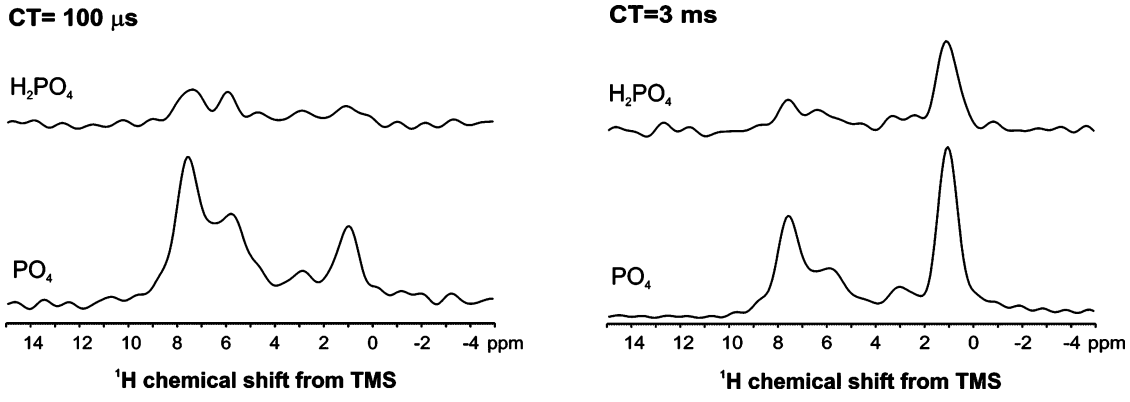

Figure 8. F1 cross-sections of the 2D $^{1}H\{FS\text{-}LG\}-^{31}P$ HETCOR NMR spectra of $(C_6H_{13}NH_3)[Ti(HPO_4)(PO_4)]\cdot H_2O$.

P−OH, and *n*-hexylammonium residues are closer than the alkyl chain protons to the two phosphorus sites. A second important observation is that, at the short contact time of 100 μs, the F1 cross-section taken through the ^{31}P (HPO_4^{2-}) peak at ca. −13.5 ppm reveals a H_2O/P−OH ^{1}H peak as intense as the N−H resonance. In contrast, the F1 cross-section taken through the ^{31}P peak at ca. −26.5 ppm exhibits a much stronger N−H proton resonance. Hence, the ^{1}H−^{31}P HETCOR NMR evidence indicates that the HPO_4^{2-} environment is closer than the PO_4^{3-} site to the water molecules, as expected.

Conclusion

γ-Titanium phosphate compounds intercalated with *n*-alkylamine may be used as precursors in pillaring reactions, because of their water stability, suitable interlayer distance, moderate affinity of the intercalated species toward the host active centers, and an adequate occupied interlayer volume. Despite the many potential applications of these materials, their detailed structural features have remained poorly understood. In this work, we have combined chemical information, spectroscopic and powder XRD data, and modeling studies to propose the first structural model of an organically templated titanium phosphate, $(C_6H_{13}NH_3)[Ti(HPO_4)(PO_4)]\cdot H_2O$. In particular, this case study provides an interesting example of how to combine powder XRD, modeling, and solid-state NMR to elucidate the structure of organic−inorganic hybrid materials.

Acknowledgment. This work was partially supported by MEC (Spain), Research Projects MAT2003-02940 and MCT-03-ACC-HP2002-0060. We also thank FEDER, POCTI (Portugal), and the Portuguese Foundation for Science and Technology (FCT) for financial support and for Ph.D. scholarship SFRH/BD/13858/2003 (to L.M.).

Supporting Information Available: TG, DTG, DSC curves, and the FTIR spectrum of $(C_6H_{13}NH_3)[Ti(HPO_4)(PO_4)]\cdot H_2O$, and SEM images of the title material stabilized in air at ambient temperature, treated at 400 °C, and stabilized at ambient temperature in a saturated atmosphere of *n*-hexylamine (60 days) (Word, PDF). This material is available free of charge via the Internet at http://pubs.acs.org.

CM051447F